MAGNETISM OF R-Co (R = Gd, Tb) FILMS WITH HIGH CONCENTRATION OF RARE EARTH ELEMENTS

© 2025 V. O. Vas'kovskiy[a,b,*], E. V. Kudyukov[a], A. N. Gorkovenko[a], A. N. Nizaev[a], A. V. Svalov[a], M. A. Semkin[a,b], V. N. Lepalovskij[a]

[a]*Ural Federal University, Ekaterinburg, Russia*

[b]*M.N. Mikheev Institute of Metal Physics of the Ural Branch of the Russian Academy of Sciences, Ekaterinburg, Russia*

**e-mail: Vladimir.Vaskovskiy@urfu.ru*

Received November 15, 2024

Revised December 14, 2024

Accepted December 30, 2024

Abstract. We studied magnetic properties of R-Co (R = Gd, Tb) films containing up to 50 at. % cobalt. The X-ray diffraction characteristics of samples, temperature dependences of magnetization for films of different compositions, concentration dependences of Curie temperature and hysteresis properties are presented. The interpretation of the established patterns is given.

Keywords: *asperomagnetism, coercive force, composition, Curie temperature, film, magnetization, rare earth elements, structure*

DOI: 10.31857/S03676765250408e8

INTRODUCTION

Films of alloys of rare-earth elements (R) with iron group metals (T) have been in the field of researchers' attention for several decades [1-6]. This is largely due to the unique possibility of realizing in them an amorphous state and, accordingly, a continuous series of solid solutions of elements bearing localized and collectivized

types of magnetism [7]. Naturally, the main attention of a large number of relevant works is focused on R-T compositions with a large content of T-elements, which possess magnetic ordering in the temperature region including room temperature [8]. In this case, the greatest interest is in R-T systems, where T= Co, Fe, and R are from among heavy rare-earth elements, primarily Gd and Tb with relatively high intrinsic temperatures of magnetic ordering. Such systems are united by the presence of two-sublattice ferrimagnetism, leading, among other things, to a specific state of magnetic compensation, but individualizes the difference in magnetic anisotropy. The latter is a consequence of peculiarities in the configuration of the 4f-electron shell of the R atoms. For Gd it is spherical, while for Tb it is characterized by a rather large orbital moment. Magnetic anisotropy in turn sets the level of magnetic hysteresis, and together they determine the options for possible technical applications of R-T media. Gd-containing films, in particular, are tried on as a magnetocaloric material [9-12] or a source of specific exchange displacement [13-15], and Tb-based films as a material for high-density information recording [16] or a magnetostrictive medium [17].

However, in recent years, interest in R-T films has also arisen in connection with the development of chiral magnetism realized in the framework of noncollinear magnetic structures, which are considered as a certain basis for the functionality of media for spintronics and MEMS devices [18-23]. Such structures are rich in pure rare earth metals, thus reflecting the indirect character of the exchange interaction in the R-ion system. This feature is translated into R-T solid solutions [24], which in wide concentration and temperature intervals are often characterized by unique noncollinear magnetism in spero-, aspero-, or sperimagnetic variants [25-28]. Moreover, in the

absence of structural order, it is usually associated with the dispersion of the axes of local magnetic anisotropy of R-ions, without taking into account the fluctuation of interatomic distances leading to exchange frustration and ultimately to the disorientation of atomic magnetic moments. In this connection, the task of comparative study of binary R-T systems that differ cardinally in the level of magnetic anisotropy arises. This work is devoted to its solution on the example of binary films Gd-Co and Tb-Co , in particular. At the same time, we have chosen the region of compositions with the prevailing content of rare-earth elements (more than 50 at. %), in which the cobalt subsystem does not contribute directly to the spontaneous magnetization and can be regarded structurally as an amorphous additive.

CHARACTERIZATION OF SAMPLES AND METHODS

The experiment was performed on films of the systems $Gd_{(100-)\,(x)}Co_{(x)}$and $Tb_{100-x}Co_{(x)}$($0 \leq x \leq 50$) obtained by magnetron sputtering in argon atmosphere at the AJA Orion-8 facility in the co-sputtering mode of single-component Gd, Tb, and Co targets. The operating pressure of argon was $2 \cdot 10^{-3}$Torr, the pressure of residual gases did not exceed $5 \cdot 10^{(-)\,(7)}$Torr. The substrates were Corning cover glasses, in the plane of which a homogeneous magnetic field (process field) of 250 E was present during film deposition. The nominal thickness of the films was 100 nm. All of them had a protective coating in the form of a surface layer of Ta with a thickness of 5 nm. The composition of the samples was varied by changing the ratio of deposition rates of different metals and monitored with a Nanohunter X-ray fluorescence analyzer. The structural state attestation was performed on a PANalytical Empyrean X-ray diffractometer in Co_Kradiation$_\alpha$. Information on magnetic properties in the

temperature range 5-350 K and in magnetic fields of up to 70 kE was obtained using the VSM option on the PPMS DynaCool measuring complex.

Fig. 1 shows diffractometry results illustrating characteristic structural features of films of two binary systems Gd-Co (Fig. 1a) and Tb-Co (Fig. 1b). For better clarity, the atomic interplanar distance *d*, whose values were obtained by recalculating the diffraction angles using the Wolf-Bregg formula for the radiation wavelength$\lambda_{CoK\alpha 1} \approx$ 0.17890 nm, was used as an argument in diffractograms. The dots denote experimental intensity values, the lines denote the results of fitting modeling performed by the Le-Bail method [29] using the FullProf Suite software package [30], and the vertical segments reflect the ratio of line intensities for media with isotropic orientation of GPU- and HCC-crystallites. It follows from the above data that at a certain external difference between the diffractograms of the two systems, they demonstrate the similarity of the structural state of films of pure rare earth elements and trends in its modification by the introduction of Co.

The main diffraction lines of both Gd and Tb are identified within the GPU-structure with pronounced signs of crystal texture types (100) and (002). Moreover, in the Tb film the first type of texture predominates, while in the Gd film they are approximately equal. At the same time, on both diffractograms in more (for Gd) or less (for Tb) clearly reveals a line indicating the presence of crystallites with HCC lattice textured by type (111). It is well known that heavy R-metals at room temperature are characterized by a GPU crystal structure. However, there is evidence that in the film state both Gd and Tb, can have a cubic modification [27, 28]. Nevertheless, it is difficult to give an unambiguous interpretation of this fact because of the possible

presence in the films of traces of oxides of the $R_{(2)}O_3$ type, having practically the same crystal structure. This, in particular, illustrates Table 1, which reflects the literature data on the structure parameters of pure metals, their oxides, as well as the results of the described experiment. Still, the indirect evidence, which will be mentioned below, allows us to interpret the situation in favor of the cubic metallic phase. Along with the noted ambiguity on the carrier of the HCC lattice, it can be stated that within the framework of the GPU structure, the unit cell parameters of the attested films and those given by other authors are quite close and reflect the tendency to the growth of the unit cell volume during the transition of R-elements from the massive to the film state.

When considering the diffractogram of the Gd film, a broad maximum in the region of localization of its main reflexes also attracts attention. A similar but less pronounced feature is also present in the diffractogram of the Tb film. This indicates the presence of a significant X-ray amorphous component in the samples, which, recall, are metal films on glass substrates. At first glance, it seems natural to attribute it entirely to the substrate, and the quantitative difference in the diffuse signal for samples with different R to the fact that Tb has a higher X-ray scattering capacity than Gd [36]. However, we believe that this halo is formed not only by the amorphous substrate but also by the metallic X-ray amorphous phase, which is very likely to be present in the films. Due to the small volume, it is not possible to directly isolate this contribution, and the corresponding conclusion is made on the basis of the subsequent analysis of magnetic properties. It is performed on the basis of the fact that films of pure Gd and Tb are characterized by structural heterogeneity and include in significant amounts at

least two crystalline phases with hexagonal and cubic symmetry and a phase characterized as X-ray amorphous.

As can be seen from Fig. 1, the diffraction pattern of pure metal films undergoes dramatic changes upon introduction of Co. The main tendency consists in the decrease of intensity of all revealed diffraction lines, which ends with their complete disappearance at the concentration of Co more than 20 at. %. 20 at. %. Thus, one can conclude about amorphization of the films, which is attributed to a significant difference in the atomic radii of Co and R-elements and low mobility of metal atoms on the substrate [1]. However, the diffractograms themselves do not provide information on the change in the fraction of the X-ray amorphous phase, as already noted, due to the shading effect of the amorphous substrate. Note also that the line attributed to the HCC structure is transformed on a par with the lines of the GPU structure, indicating the amorphization of the HCC phase, which can be considered as an indirect confirmation of its neoxide nature.

MAGNETIC PROPERTY ANALYSIS

The temperature dependences of the magnetization $M(T)$ shown in Figs. 2a and 2b contain significant information on the magnetism of the Gd-Co and Tb-Co film systems. All of them were measured when the films were heated from 5 K in a magnetic field of 100 E strength. The samples were cooled down to the initial state in magnetic field of 70 kE, which, like the measurement field, was co-directional with the process field in which the films were deposited. Let us first turn to the $M(T)$ dependences of pure R-elements. They demonstrate two features that fundamentally distinguish them

from the dependences $M(T)$, peculiar to these metals in the massive state. First, these curves have an atypical for ferromagnetics concave form. The observed course of magnetization can be qualitatively justified on the basis of ideas about the highly dispersed and inhomogeneous structural state of films, as well as the dependence of the Curie temperature on the size of nanocrystallites. In this setting, the experimental values of Curie temperatures (T_C~ 280 and 210 K), which do not differ much from the characteristics of the massive state of Gd and Tb (293 and 221 K), can be associated with the largest crystallites, which probably give reflexes on diffractograms. Smaller, apparently, X-ray amorphous structural elements are characterized by a set of Curie temperatures depending on their size and gradually leave the magnetically ordered state as they are heated. In this case, the concave character of $M(T)$ provides the corresponding size distribution of nanocrystallites.

Second, the experimental values of the magnetization $M(T= 5$ K) for both Gd (460 Gs) and Tb (420 Gs) are far from the values of the spontaneous magnetization $M_{(s)\ of}$these metals (1950 and 2700 Gs). Taking into account the protocol of measurements, we can conclude that this is not a consequence of self-demagnetization of the samples, but is due to the inhomogeneity of their magnetic structure. In other words, asperomagnetism takes place, which in alloys of heavy rare-earth elements was observed earlier [22] and was associated with the dispersion of the light magnetization axes within microcrystalline or even amorphous structures. However, for Gd, which has no orbital moment and does not carry significant magnetic anisotropy, the presence of signs of asperomagnetism should have a different interpretation. In our opinion, the reason for the inhomogeneity of the magnetic structure may be interatomic exchange

frustration, which is understood as the presence and impossibility of satisfying all multipolar exchange bonds in a magnetic system. Taking into account the RKKI exchange mechanism, it can be assumed that the frustrated state of Gd arises as a result of fluctuations in the interatomic distances occurring due to the highly dispersed structure of the films. Ideally, such a mechanism should pressurize the spheromagnetic state. Perhaps, in this case, the asperomagnetism has an effective character, being a superposition of the ferromagnetism of the crystalline phase and the spheromagnetism of the X-ray amorphous structural component. Obviously, such a mechanism should also take place in Tb films. But this does not exclude the disorienting role of magnetic anisotropy in the formation of their magnetic structure. Perhaps, it is the superposition of two dispersion mechanisms that leads to the fact that in Tb films the ratio $M(T= 5$ K)/ $M_s$is 0.15, which is much smaller than in Gd films (0.24).

Turning to the temperature dependences of the magnetization of the binary systems $Gd_{100-x}Co_x$and $Tb_{100-x}Co_x$, we can state the commonality of the trends of their changes with increasing Co content. And these changes are significant and consist in the growth of $M(T= 5$ K), formation of convex form of $M(T)$ curves and non-monotonic change of Curie temperature. Within the framework of the above treatment of the properties of Gd and Tb films, these changes can be considered as a consequence of the increase in the homogeneity of the magnetic structure, i.e., the transition from asperomagnetic to ferromagnetic ordering. Recall that, according to diffractometry data, the addition of Co even in relatively small amounts leads to a decrease in the fraction of the crystalline phase, and at $x> 20$ at. % the films become X-ray amorphous (see Fig. 1). In accordance with this, the high-temperature regions on the M(T)

dependences also disappear, thus confirming their connection with the crystalline phase. Since the modification of the curves M(T) is not limited here, it can be assumed that structural transformations from some intermediate nanocrystalline to the final amorphous state also occur within the X-ray amorphous phase. In the amorphous phase, the dispersion in the interatomic distances within the rare-earth subsystems decreases, i.e., a more homogeneous atomic structure is formed in a certain sense. This reduces the exchange frustration and leads the $M(T)$ dependence to a ferromagnet-like form. From the comparison of Figs. 2a and 2b, we can also conclude that in the Tb-Co system the mentioned structural transformations, which cause the observed transformation of $M(T)$ curves, are stretched over a larger concentration range, i.e. indirectly they contain structural information, which cannot be obtained directly from diffractograms.

The above-mentioned non-monotonicity in the concentration variation of the Curie temperature is clearly illustrated in Figs. 3a and 3b (curves 1). As can be seen, the increase of Co content up to ~ 20 at. % causes a significant decrease of T_C, and further increase of x leads to its no less strong increase in films of both systems. In our opinion, such variation of physical properties, as it often happens, is caused by the competition of two opposite tendencies. On the one hand, amorphization, due to its accompanying exchange frustration, sets a decreasing trend of $T_{(C)}(x)$ dependence, which is likely to be exhausted at $x \approx 20$ at. %, when the amorphous phase becomes dominant. On the other hand, the hybridization of the electronic structures of Co and R-elements seems to follow the path of strengthening the efficiency of the indirect exchange interaction in the system of rare-earth ions, accompanied by an increase in

T_C. The qualitative similarity of the $T_{(C)}(x)$ dependence for films with highly anisotropic Tb and with Gd, which has no orbital moment, can be regarded as an argument in favor of the hypothesis about the important role of the exchange contribution to the mechanism of formation of the asperomagnetic state.

In Fig. 3 also shows the concentration dependences of the coercivity $H_{(c)}$ of $Gd_{(100-x)}Co_x$ films (Fig. 3a) and $Tb_{100-x}Co_{(x)}$ films (Fig. 3b) determined from the hysteresis loops at T= 5 K. In this respect, the two systems show quite different patterns. In Gd-based films, with increasing x , there is first a sharp (up to x~ 20 at. %) and then a smoother decrease in H_c. It is noteworthy to note the manifestation of significant hysteresis (H_c= 600 E) in pure Gd films. Since the magnitude of the coercive force is closely related to the level of magnetic anisotropy in the medium, we can state the existence of such anisotropy in Gd, despite the lack of appropriate assumptions due to the sphericity of its electron shell. Moreover, this anisotropy has a crystalline nature, since amorphization, occurring with increasing x, reduces H_c, and hence the magnitude of magnetic anisotropy to a minimum. In contrast, pure Tb films have a high coercivity, which, interestingly enough, becomes even larger when Co is added. It follows that in this case amorphization does not lead to a weakening of magnetic anisotropy, rather it increases. The reason for this can be sought, for example, in the weakening of exchange frustration, which is responsible for asperomagnetism, i.e., the isotropic distribution of local magnetically reduced moments. As a result, the dispersion of local light magnetization axes comes to the fore, which, under the corresponding magnetic prehistory, sets the half-space distribution of magnetic moments. These moments do

not have neighbors with opposite orientation and do not experience a "tipping" effect from their side.

CONCLUSION

The presented experimental data and their analysis show that films based on rare-earth metals with significantly different electron shell configurations (Gd, Tb) exhibit similar regularities of crystal structure formation, magnetic ordering, and a number of magnetic properties. They consist in the structural heterogeneity of pure rare-earth metal films, their amorphization within the binary systems Gd-Co and Tb-Co, the presence of asperomagnetism, non-monotonic concentration variation of the Curie temperature. In this case, the exchange frustration of magnetic moments in Gd-Co films is responsible for the presence of asperomagnetism, to which the dispersion of local anisotropy axes in Tb-Co films is added. Increasing the Co concentration increases the degree of amorphization, promotes the formation of a homogeneous atomic structure and weakens the exchange frustration. In Gd-Co films, this leads to ferromagnetic ordering, while in the asperomagnetism of Tb-Co films it increases the relative role of the dispersion of local magnetic anisotropy axes. The differences in the magnetic structure of the films of the two systems determine the fundamental difference in the concentration change of their hysteresis properties.

ACKNOWLEDGEMENT

The authors are grateful to E.A. Kravtsov and M.E. Moskalev for their help in structural attestation of the films. Moskalev for their help in the structural attestation of the films.

FUNDING

This work was supported by the Russian Science Foundation, project No. 24-22-00173.

REFERENCES

1. *Taylor R.C., Gangulee A.* // J. Appl. Phys. 1976. V. 47. No. 10. P. 4666.

2. *Drovosekov A.B., Kholin D.I., Kreinies N.M.* // JETP. 2020. V. 131. No. 1. P. 149.

3. *Morshed M.G., Khoo K.H., Quessab Y. et al.* // Phys. Rev. B. 2021. V. 103. Art. No. 174414.

4. *Pashueva I.M., Bondarev A.V., Bataronov I.L.* // Bull. Russ. Acad. Sci. Phys. 2022. V. 86. No. 6. P. 569.

5. *Kudyukov E.V., Vas'kovskiy V.O., Svalov A.V. et al.* // J. Magn. Magn. Mater. 2023. V. 565. Art. No. 170254.

6. *Yurlov V.V., Zvezdin K.A., Zvezdin A.K.* // Bull. Russ. Acad. Sci. Phys. 2024. V. 88. No. 1. P. 97.

7. *Yang X., Miyazaki T.* // J. Appl. Phys. 1988. V. 64. P. 5489.

8. *Kobliska R.J., Gangulee A., Cox D.E., Bajorek C.H.* // IEEE Trans. Magn. 1977. V. 13. No. 6. P.1767.

9. *Koplak O.V., Kashin S.N., Korolev D.V. et al.* // Phys. Solid State. 2023. V. 65. No. 3. P. 415.

10. *Kuznetsov M.A., Drovosekov A.B., Fraerman A.A.* // JETP. 2021. V. 132. No. 1. P. 79.

11. *Svalov A.V., Arkhipov A.V., Lepalovskii et al.* // Phys. Solid State. 2021. V. 63. P. 1553.

12. *Tereshina I.S., Ovchenkova I.A., Politova G.A., Pankratov N.Yu.* // Bull. Russ. Acad. Sci. Phys. 2023. V. 87. No. 3. P. 304.

13. *Svalov A.V., Kurlyandskaya G.V., Vas'kovskiy V.O.* // Appl. Phys. Lett. 2016. V. 108. Art. No. 063504.

14. *Drovorub E.V., Prudnikov V.V., Prudnikov P.V.* // Bull. Russ. Acad. Sci. Phys. 2022. V. 86. No. 2. P. 109.

15. *Svalov A.V. Kudyukov E.V., Lepalovskij V.N. et al.* // Curr. Appl. Phys. 2021. V. 23. P. 68.

16. *Wang J., Gan J.A., Wong Y.C., Berndt C.C.* Magnetic Thin Films: Properties, Performance and Applications. N.Y.: Nova Science Publ. Inc, 2011. 409 p.

17. *Chelvane J.A., Sherly A., Palit M. et al.* // J. Mater. Sci. Mater. Electron. 2019. V. 20. P. 8989.

18. *Basha M.A., Prajapat C.L. Bhatt H. et al.* // J. Appl. Phys. 2020. V. 128. Art. No. 103901.

19. *Antropov N.O., Kravtsov E.A., Khaidukov Yu.N. et al.* // JETP Lett. 2018. V. 108. No. 5. P. 341.

20. *Streubel R., Lambert C.H., Kent N. et al.* // Adv. Mater. 2018. V. 30. Art. No. 1800199.

21. *Yang D.Z., You B., Zhang X.X. et al.* // Phys. Rev. B. 2006. V. 74. Art. No. 024411.

22. *Bai X.J., Du J., Zhang J. et al. //* J. Phys. D. Appl. Phys. 2008. V. 41. Art. No. 215008.

23. *Stanciu A.E., Schinteie G., Kuncser A. et al.* // J. Magn. Magn. Mater. 2020. V. 498. Art. No. 166173.

24. *Uchiyama S.* // Mater. Chem. Phys. 1995. V. 42. P. 38.

25. *Tufaile P.B., Santos A.D.P.* Magnetism, magnetic materials and their applications. Switzerland: Trans Tech Publications Ltd, 1999. P. 120.

26. *Hussain R., Aakansha, Brahma B. et al.* // J. Supercond. Nov. Magn. 2019. V. 32. P. 4027.

27. *Krnel M., Vrtnik S., Jelen A. et al.* // Intermetal. 2020. V. 117. Art. No. 106680.

28. *Sinitsyn E.V., Ryzhenko A.B.* // J. Magn. Magn. Mater. 1995. V. 147. P. 385.

29. *Le Bail A.* // Powder Diffr. 2005. V. 20. No. 4. P. 316.

30. *Rodríguez-Carvajal J.* // J. Physics B. 1993. V. 192. No. 1-2. P. 55.

31. *Zhang Y.Z., Zhang S.R., Yu D.B.* // Rare Metals. 2023. V. 42. P. 1414.

32. *Scheunert G., Ward C., Hendren W.R. et al.* // J. Phys. D. Appl. Phys. 2014. V. 47 No. 41. Art. No. 415005.

33. *Norman M., Harris I.R., Raynor G.V.* // J. Less-Common Met. 1966. V. 11 P. 395.

34. *Kashaev A.A., Ushchapovskii L.V., Il'in A.G.* // Kristallografiya. 1975. V. 20. P. 192.

35. *Spedding F.H., Sanden B., Beaudry B.J.* // J. Less-Common Met. 1973. V. 31. P. 1.

36. *Waasmaier D., Kirfel A.* // Acta Cryst. 1995. V. 51. No. 3. P. 416.

FIGURE CAPTIONS

Fig. 1. Experimental (crosses) and calculated (lines) X-ray diffraction patterns of $Gd_{100-x}Co_{(x)\,(a)}$) and $Tb_{100-x}Co_{(x)\,(b)}$) films. The indices (*hkl*), the most intense, Bragg reflexes of the GPU and HCC phases are indicated in parentheses. Vertical lines at the bottom indicate the positions and the ratio of the intensities of the main reflexes of the GPU and HCC phases in the polycrystalline state of Gd (a) and Tb (b).

Fig. 2. Temperature dependences of the magnetization of films of binary systems $Gd_{100-x}Co_{(x)\,(a)}$) and $Tb_{100-x}Co(_{x)\,(b)}$of different compositions.

Fig. 3. Concentration dependences of Curie temperature $T_{(C)\,(}$curves 1) and coercivity $H_{(c)\,(}$curves 2) at T= 5 K for $Gd_{(100-x)}Co_{(x)\,(}$a) and $Tb_{(100-x)}Co(_{x)\,(b)}$) films.

Table 1. Parameters of unit cells of GPU and HCC modifications of Gd and Tb in massive and film states obtained from literature sources and determined experimentally.

Composition and type of environment	a_{GPU}, nm	c_{GPU}, nm	a_{HCC}, nm
Literature			
Gd (array) [33]	0.3634± 0.0002	0.5781± 0.0001	-
Gd (film) [32]	0.366± 0.002	0.582± 0.002	0.533± 0.001
$Gd_{(2)\,O(3)\,(}$array) [35]	-	-	0.531± 0.002
Tb (array) [35]	0.3606± 0.0004	0.5697± 0.0006	-
Tb (film) [32]	0.364± 0.002	0.576± 0.002	0.527 ± 0.001
$Tb_{(2)\,O(3)\,(}$array) [34]	-	-	0.528± 0.002
Results of fitting analysis of diffractograms of investigated samples			
Gd (film)	0.3649± 0.0005	0.5834± 0.0005	0.5326± 0.0004
Tb (film)	0.3632± 0.0005	0.5777± 0.0005	0.5310± 0.0005

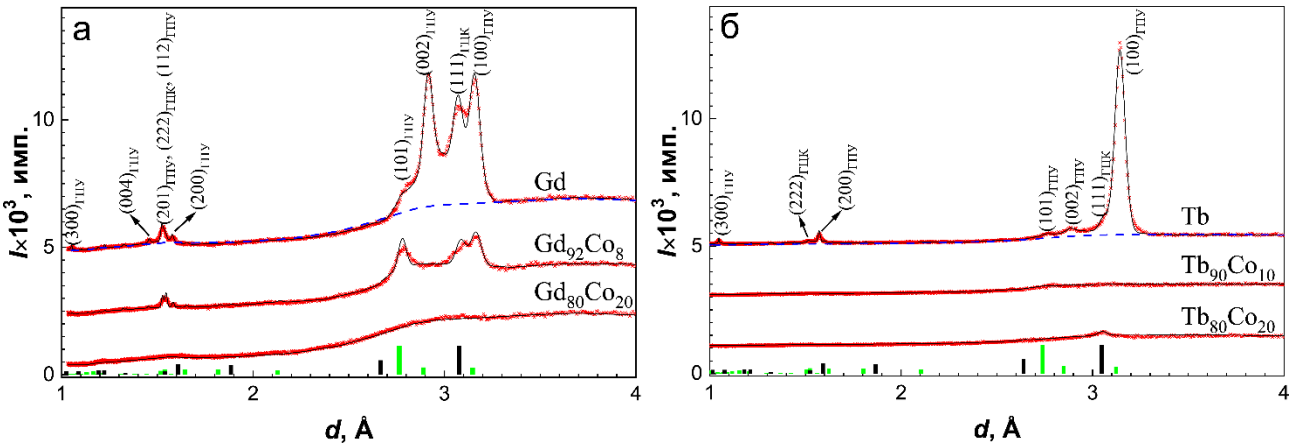

Fig. 1.

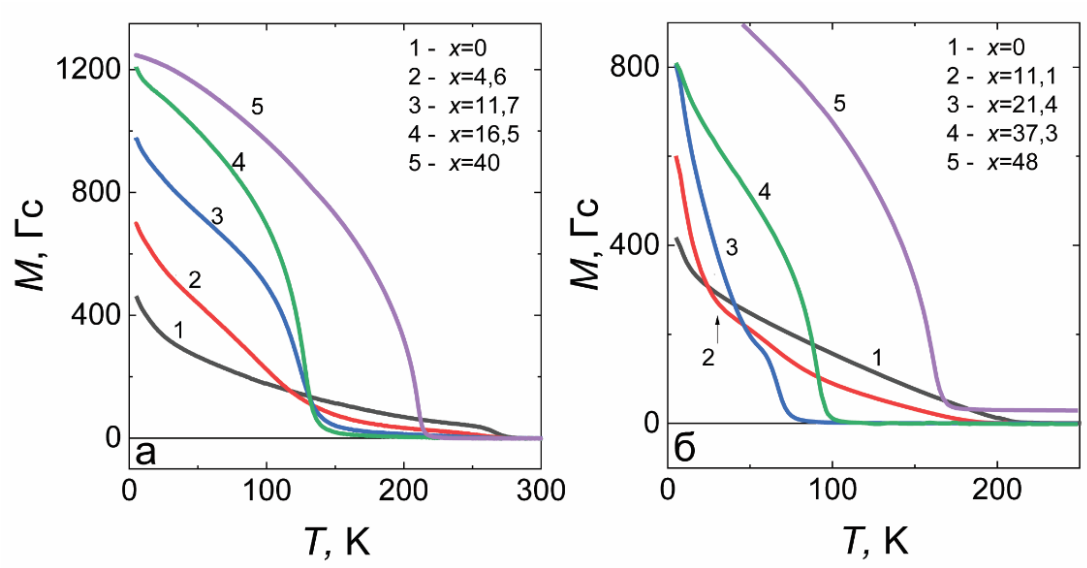

Fig. 2.

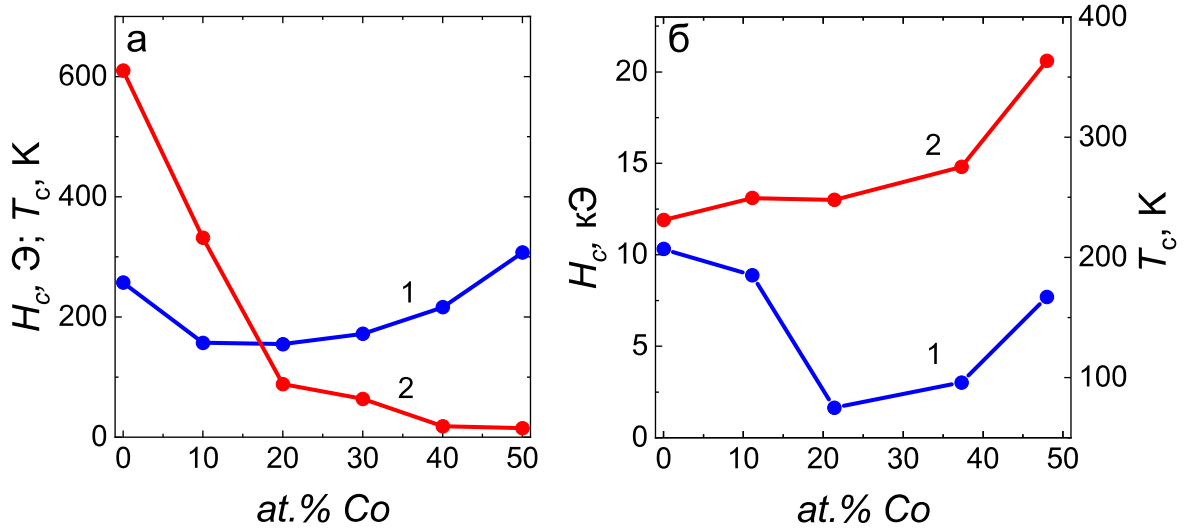

Fig. 3.